BNL-207826-2018-JAAM

Use of the drift-time method to measure the electron lifetime in long-drift-length CdZnTe detectors

A. E. Bolotnikov,

To be published in "Journal of Applied Physics "

September 2016

Nonproliferation and National Security Department

Brookhaven National Laboratory

U.S. Department of Energy

USDOE National Nuclear Security Administration (NNSA), Office of Nonproliferation and Verification Research and Development (NA-22)

DISCLAIMER

Use of the drift-time method to measure the electron lifetime in long-drift-length CdZnTe detectors

A. E. Bolotnikov,[1] G. S. Camarda,[1] E. Chen,[2] R. Gul,[1] V. Dedic,[1,3] G. De Geronimo,[1] J. Fried,[1] A. Hossain,[1] J. M. MacKenzie,[2] L. Ocampo,[1,4] P. Sellin,[5] S. Taherion,[2] E. Vernon,[1] G. Yang,[1] U. El-Hanany,[2] and R. B. James[1,6]

[1]*Brookhaven National Laboratory, Upton, New York 11793, USA*
[2]*Redlen Technologies, Saanichton, British Columbia V8M 0A5, Canada*
[3]*Institute of Physics of Charles University, Prague 12116, Czech Republic*
[4]*Department of Mechanical and Nuclear Engineering, Pennsylvania State University, University Park, Pennsylvania 16802, USA*
[5]*Department of Physics, University of Surrey, Surrey GU2 7XH, United Kingdom*
[6]*Science and Technology Directorate, Savannah River National Laboratory, Aiken, South Carolina 29808, USA*

(Received 31 May 2016; accepted 29 August 2016; published online 14 September 2016)

The traditional method for electron lifetime measurements of CdZnTe (CZT) detectors relies on using the Hecht equation. The procedure involves measuring the dependence of the detector response on the applied bias to evaluate the $\mu\tau$ product, which in turn can be converted into the carrier lifetime. Despite general acceptance of this technique, which is very convenient for comparative testing of different CZT materials, the assumption of a constant electric field inside a detector is unjustified. In the Hecht equation, this assumption means that the drift time would be a linear function of the distance. This condition is not fulfilled in practice at low applied biases, where the Hecht equation is most sensitive to the $\mu\tau$ product. As a result, researchers usually take measurements at relatively high biases, which work well in the case of the low $\mu\tau$-product material, $<10^{-3}$ cm^2/V, but give significantly underestimated values for the case of high $\mu\tau$-product crystals. In this work, we applied the drift-time method to measure the electron lifetimes in long-drift-length (4 cm) standard-grade CZT detectors produced by the Redlen Technologies. We found that the electron $\mu\tau$ product of tested crystals is in the range 0.1–0.2 cm^2/V, which is an order of the magnitude higher than any value previously reported for a CZT material. In comparison, using the Hecht equation fitting, we obtained $\mu\tau = 2.3 \times 10^{-2}$ cm^2/V for a 2-mm thin planar detector fabricated from the same CZT material. *Published by AIP Publishing.*
[http://dx.doi.org/10.1063/1.4962540]

I. INTRODUCTION

The charge-carrier lifetime is an important characteristic of radiation detectors operating in the charge-collection mode. Lifetime is a measure of the charge-carriers' trapping rate as they drift from the point of origin toward the collecting electrodes, and the lifetime value is critical for achieving high energy resolution.

The conventional method for electron-lifetime measurements in CdZnTe (CZT) detectors relies on using the Hecht equation.[1,2] The procedure involves measuring the dependence of the detector response (the photopeak position in the pulse-height spectra) on the cathode bias and fitting this dependence using the Hecht equation to evaluate the $\mu\tau$ product, which in turn can be converted into the carrier lifetime assuming a constant drift velocity (or a constant electric field) in the detector and a known electron mobility, $\sim$1000 cm^2/V-s. Despite general acceptance of this technique, which is very convenient for quick evaluation of CZT samples, the assumption of a constant electric field is not always justified. In the Hecht equation, the assumption of a constant electric field means that the drift time would be an inverse function of the applied bias. However, this condition is not fulfilled at low biases—the region where the Hecht equation is most sensitive to the $\mu\tau$ product. Moreover, at low biases, the measurements are likely to be affected by ballistic deficit, electron diffusion, surface recombination, and low signal-to-noise ratio. This dilemma—the necessity of taking measurements at low biases, on one side, and significant systematic errors associated with low biases, on the other—has no simple solution in the case of the high $\mu\tau$ product CZT material, $>10^{-3}$ cm^2/V, especially for thick detectors.

A modified Hecht equation was proposed for pixelated detectors,[3] which allows using only two charge amplitudes measured at two voltages (instead of fitting the charge collection efficiency curve over a broad range of biases). As in the case of the traditional Hecht-equation method, it also suffers from systematic errors, which may explain the relatively lower $\mu\tau$ products reported in the above work.

A different approach for the electron lifetime measurement was developed by researchers working with detectors of noble gases and of liquids. These detectors measure carrier drift times and collect charge signals in long-drift-distance ionization chambers. Two examples of the implementation of this technique are a 7-cm long ionization chamber that was employed to capture signals generated by cosmic muons, which were then analyzed to evaluate the electron drift times and electron trapping in high-pressure Xe detectors,[4] and a

20-cm long double-gridded drift ionization chamber that was used by the ICARUS team[5] to measure electron drift times and trapping in a liquid Ar time projection chamber. A common feature of those methods is that they rely on the direct measurement of the electron drift times that typically gives a low estimate for the electron lifetime (as in the first example), which can be further refined by using the ratio between the amounts of the collected and the initially generated carriers (in the second example). For this reason, we group these measurement approaches and call them the drift-time method. It addresses both problems mentioned above; it is independent of the electric-field distribution in the crystal, and it eliminates ballistic deficit effects caused by the use of a shaping amplifier.

The main idea of this method is to measure long drift times (as long as practically possible) for electron clouds by using thick detectors and applying low biases. If a fraction of the electron charge loss across a detector is small (less than a few percent), then the electron-cloud drift time method will give a more reliable estimate for the electron lifetime and provide better practical characterization of the charge collection than the Hecht method. In this paper, we describe the implementation of the drift-time method to evaluate the electron $\mu\tau$ product by using the cathode and anode signal waveforms captured from thick (40-mm-long) virtual Frisch-grid detectors biased at low voltages.

II. EXPERIMENTAL

We used long-drift $6 \times 6 \times 40\,\text{mm}^3$ virtual Frisch-grid detectors assembled from CZT crystals supplied by the Redlen Technologies, whose performances have been previously tested and reported elsewhere.[6] Three detectors chosen from this batch were mounted on the fanout boards as illustrated in Fig. 1. The anode and the cathode were connected using CuBe spring contacts attached to the top and bottom surfaces of the detector, as previously described.[6] The detectors were placed vertically with the anode side down on the substrate's pad, while the position sensing pads with the pigtails were directly soldered to the surrounding pads, which were kept at a ground potential during these measurements. The fanout substrate was plugged into a motherboard that contained two eV-5092 hybrid charge-sensitive preamplifiers to read out the cathode and anode signals generated by gamma rays from a ^{137}Cs source. The output signals were captured with a HDO8000 Teledyne LeCroy oscilloscope. The high-level triggers were set for the cathode channels to select mainly the photopeak events interacting close to the cathode. First, we applied the highest bias (−5000 V) to the cathode and measured the amplitudes of the anode signals equivalent to the total energy deposited by a 662-keV photon in a single photoabsorption event. Next, we reduced the cathode bias to the lowest value at which reliable measurements were still possible (about 200 V in this case). We saved the captured waveforms and analyzed them offline using the digital pulse processing algorithm developed for this type of detectors.[7] For each recorded event, we evaluated the drift times and the ratio of the anode signals measured at high and low biases, 5000 V and 200 V, and converted them into the electron lifetime, τ, using the formula

$$\tau = t/ln\left(\frac{Q_0}{Q}\right), \tag{1}$$

where Q_0 is evaluated at 5000 V.

Alternatively, one can perform these operations directly using the oscilloscope's functions.

The main source of uncertainties during the long-drift and low-bias measurements is the decay time of the charge-sensitive preamplifier, ∼1 ms, and the electron detrapping. Digital pulse processing helps minimizing the influence of these effects, which we discuss in Section III.

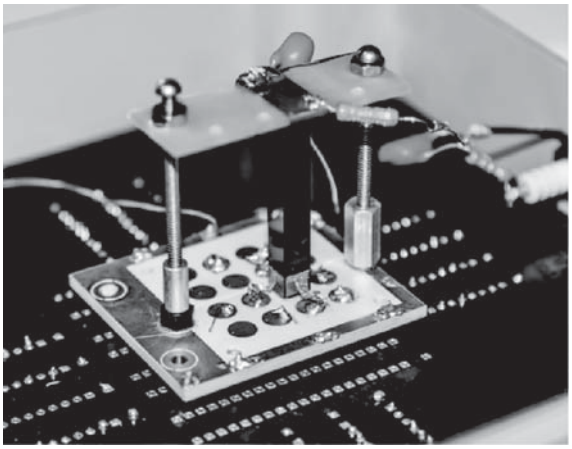

FIG. 1. A photograph of the $6 \times 6 \times 40\,\text{mm}^3$ virtual Frisch-grid detector encapsulated into the ultra-thin polyester shell, with four shielding copper tape pads and two CuBe spring contacts (on the cathode and the anode sides), mounted on the fanout substrate plugged into the motherboard.

III. RESULTS AND DISCUSSION

We first address the uncertainties in the collected charge and drift-time measurements. Figures 2(a)–2(d) show representative waveforms of anode signals measured at 2000, 1000, 500, and 200 V. An example of the cathode signal, being used to evaluate the starting time of an electron cloud as it drifts towards the anode, is also shown in the first plot (2000 V); in the rest of the plots, the starting time is indicated by the solid line. As seen in the figures, the anode signals have two components: A fast-rising one that represents the signals induced by the originally produced electrons and a slow one—first rising and then decaying—which represents the electron detrapping and a decay slope of the preamplifier. Since the signal generated by the detrapped electrons starts right after the electron cloud reaches the anode, the fraction of the originally produced electrons reaching the anode, and the time when they reach the anode can be accurately evaluated, as illustrated in the plots of Fig. 2. An intersection of two lines extending the fast and slow slopes gives the time when the electron cloud reaches the anode, while the amplitude of the signal measured at this time gives an estimate for the collected charge. In all the above plots, except for the 200-V transients, the drift time and the collected charge amplitude can be clearly identified. In the case of the 200-V plot, there is no clear transition between the signal induced by the original

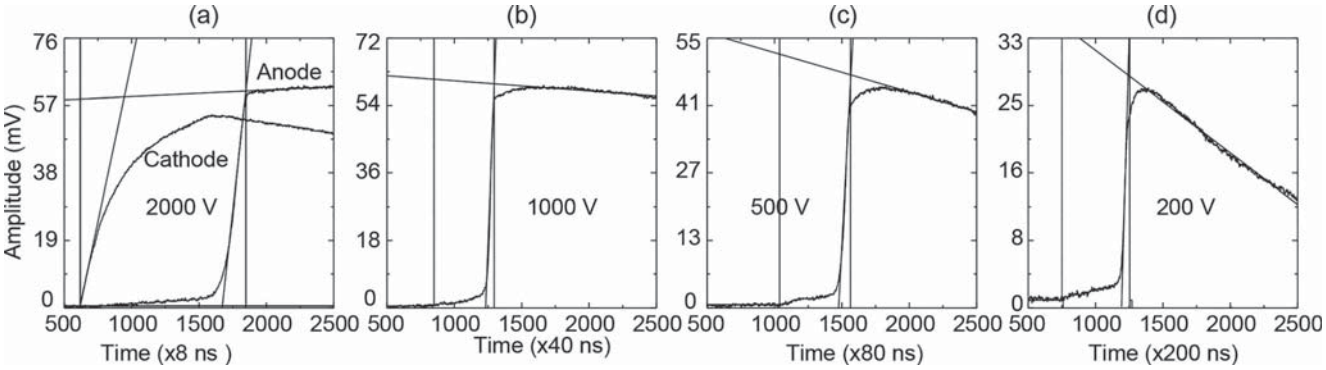

FIG. 2. Representative waveforms of anode signals measured at 2000, 1000, 500, and 200 V. An example of the cathode signal, which is used to evaluate the starting time of an electron cloud as it drifts towards the anode, is also shown in plot (a); in the rest of the plots, the starting time is indicated by the solid line. The fast-rising curve represents the signals induced by the originally produced electrons, and the slow one (first rising and then decaying) represents the electron detrapping and a decay slope of the preamplifier.

cloud and the signal induced by detrapped electrons. This procedure allowed us to minimize the effect of the detrapping on the electron lifetime measurements.

To illustrate that the electron detrapping has a small effect on our measurements, Figs. 3(a)–3(c) show distributions of the drift time, the anode amplitude, and the lifetime measured at three biases: 3000 V, 1000 V, and 200 V. The locations for the lifetime-peak maximum are nearly the same for all three biases. The broadening of the lifetime distribution at high bias indicates the fact that $ln(Q_0/Q)$ becomes very sensitive to any small variations of the ratio Q_0/Q, when the value is close to 1. Q_0 is evaluated at 5000 V.

Figure 4 shows distributions of the drift time, the anode amplitude, and the lifetime measured for one of the detectors. Similar distributions were measured for all three detectors. The average electron lifetimes were found to be in the range 90–110 μs. However, for some events, the electron lifetimes were as long as 240 μs. Such events are seen as the long tail in the lifetime distribution. These variations of the lifetime can be explained by the impact of extended (prismatic) defects present in the tested crystals.[6]

Figures 5(a) and 5(b) illustrate the cathode and anode signals of two captured events: from the tail (a) and around the photopeak (b) of the lifetime distribution shown in Fig. 5(c).

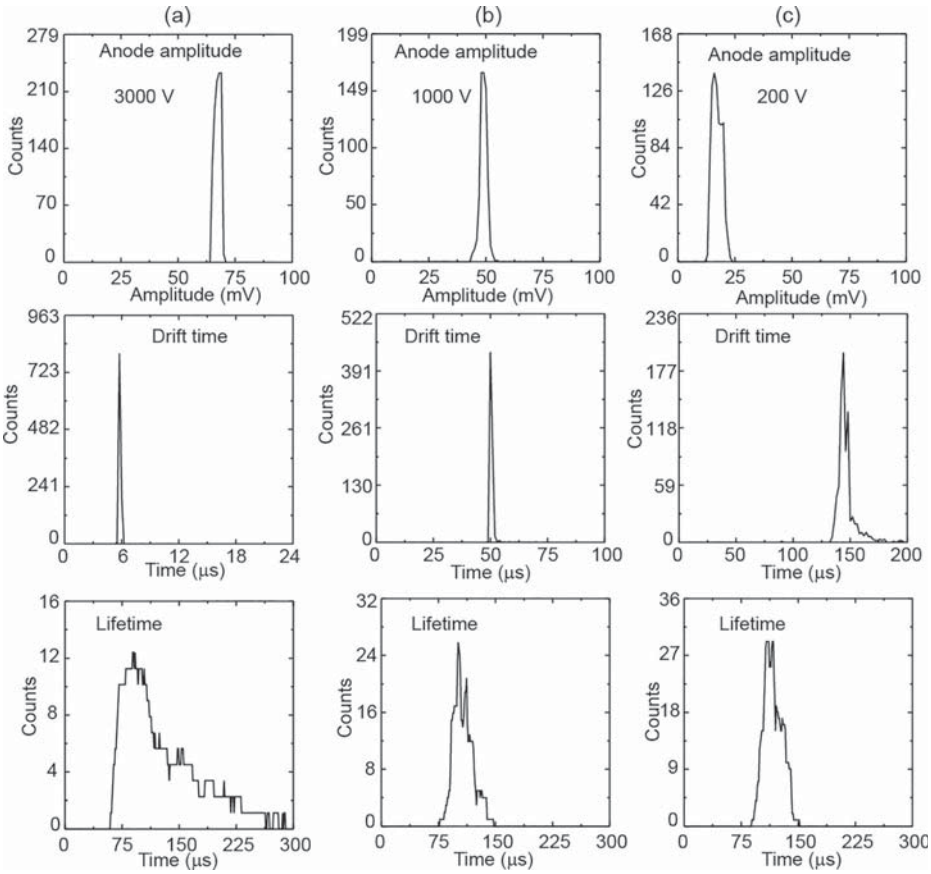

FIG. 3. Distributions of the drift time, the anode amplitude, and the lifetime measured at three biases: 3000 V, 1000 V, and 200 V.

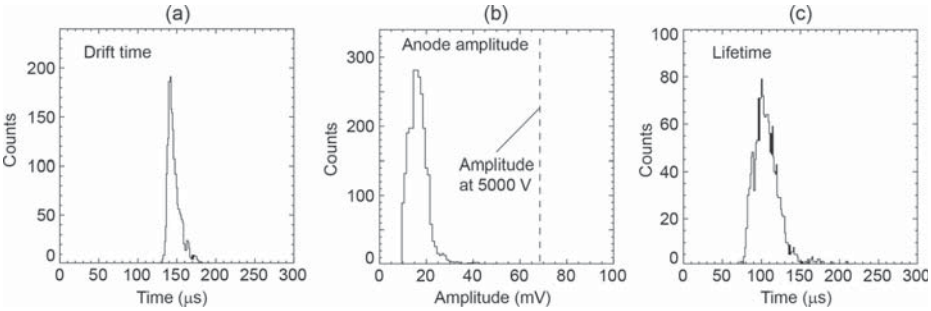

FIG. 4. Distributions of drift time, anode amplitude, and lifetime measured with one of the detectors (Q_0 is evaluated at 5000 V).

The fitting results are also shown in Fig. 5. The intersections of the two fitting lines of the anode signals were taken as the arrival times of the electron cloud to the anode. The intersections of the cathode fitting lines and the baseline were taken as the moments when interactions occur. For example, in the events from the tail (Fig. 5(a)), the measured drift times were 3.3 μs and 135 μs at 5000 V and 200 V, respectively. For comparison, assuming a constant electric field along the detector and an electron mobility $\mu = 1000\,\text{cm}^2/\text{V s}$, then the expected drift time would be $t = L^2/\mu U$ (where L is the drift distance, and U is the applied bias) giving drift time values of 3.2 μs and 80 μs for $U = 5000$ V and 200 V, respectively. The measured value is notably longer than these values as it could be expected in the case of a non-uniform electric field. The anode amplitude measured at the highest bias corresponds to the total charge generated by the 662-keV photon, while neglecting the small charge loss at the high biases. This gives a calibration point for the electron lifetime measurements. Reducing the cathode voltage to the lowest level at which such drift-time measurements are still possible and substituting the measured amplitudes of the anode signals (69 and 38 mV at 5000 and 200 V, respectively) into Equation (1), we obtain an electron lifetime of 226 μs (which for a value of $\mu = 1000\,\text{cm}^2/\text{V-s}$ will translate to $0.2\,\text{cm}^2/\text{V}$ for the $\mu\tau$ product). For comparison, for the peak event (Fig. 3(b)), the electron lifetime was 110 μs. We note that no correction has been made for the amplitude on the anode signal related to the finite decay time of the preamplifier (1 ms). Although small, such a correction should further increase the electron lifetime estimate.

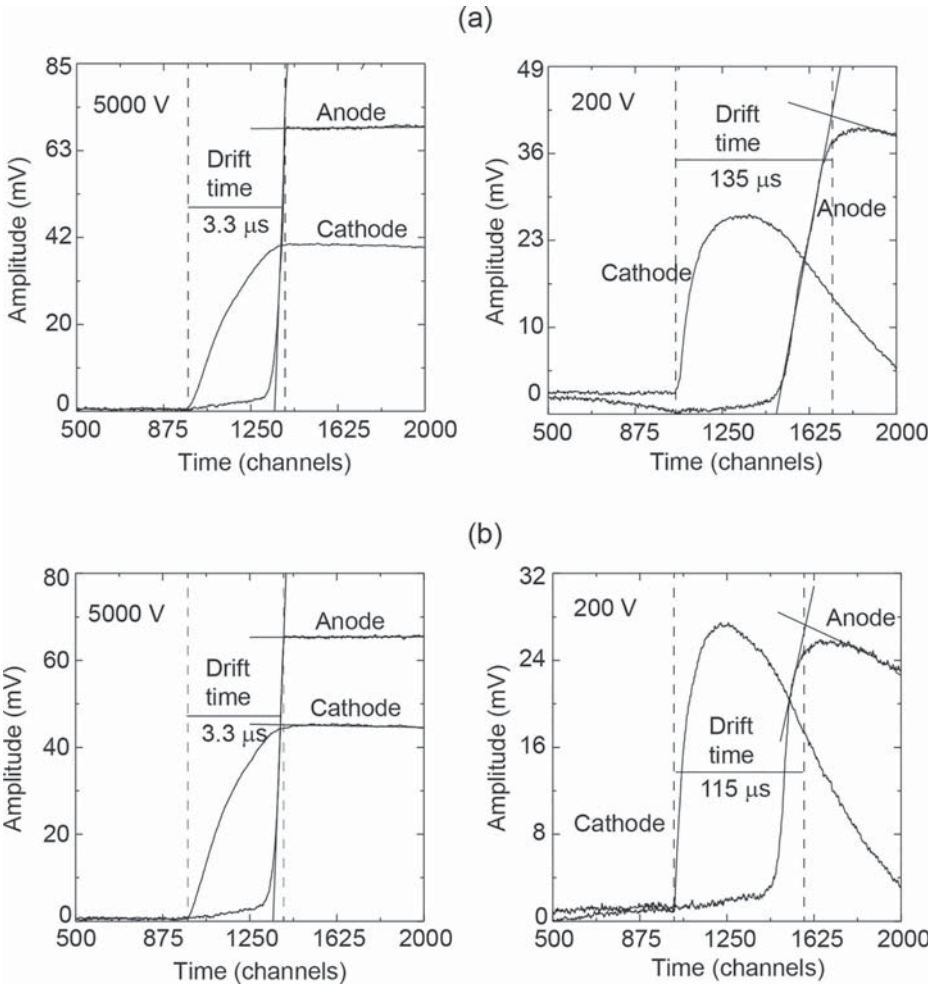

FIG. 5. Representative waveforms of the cathode and anode signals generated for events occurring near the cathode measured for two cathode biases: 5000 V (left) and 200 V (right). The time bins (channel widths) are 8 and 200 ns, respectively. The results of the fitting procedure are also shown.[7]

From the waveforms shown in Fig. 4, it is clear that a significant fraction of the charge cloud successfully drifts the full length of the detector even at very low bias voltages. With drift times in excess of 135 μs, the normal Hecht technique cannot be applied to the cathode signal for estimated mobility-lifetime products due to excessive ballistic deficit.

The evaluated electron lifetimes and the $\mu\tau$ products are one order of magnitude higher than the highest values reported for the CZT material based on fitting to the Hecht equation. In order to explain such a discrepancy, we have analyzed the applicability of the Hecht equation to the CZT material.

A common procedure for estimating carrier lifetimes by using the Hecht equation consists of fitting the measured dependences of the collected charge versus the applied bias. However, this technique, which generally provides reliable results, must be used cautiously. Since the Hecht equation has a limited range of sensitivity for accurate fitting, the measurements should be taken in the bias region where there is a sufficiently strong variation of the collected charge. The decay of the free-carrier concentration with time is described by

$$Q = Q_0 \exp\left(-\frac{t}{\tau}\right), \tag{2}$$

where τ is the electron lifetime and Q_0 and Q are, respectively, the initial number and the time-dependent number of carriers.

Usually, X-rays or alpha particles from a ^{241}Am source are used to evaluate the electron lifetimes in CZT detectors. For these sources, the electron clouds are generated near the surface of a planar detector, and they drift across the detector towards the anode. The collected charge is proportional to the amplitude of the signals measured from the anode. Assuming a uniform electric field, the drift time, t_{dr}, and the drift distance, L, are related as

$$t_{dr} = \frac{L}{\mu E} = \frac{L^2}{\mu U}, \tag{3}$$

where μ is the electron mobility, E is the strength of the electric field, and U is the applied bias. In detector-grade CZT materials, μ is 1000 cm^2/V s and is independent of the electric field strength. In planar-geometry devices, the current generated at the anode as the electron cloud drifts from the cathode towards the anode is given by

$$i(t) = Q_0 \frac{V(t)}{L} \exp\left(-\frac{t}{\tau}\right), \tag{4}$$

where $V(t)$ is the drift velocity of the electron cloud. The total collected charge at the anode after the electron cloud drifts between the cathode and the anode is given by

$$Q = Q_0 \exp\left(-\frac{L}{E\mu\tau}\right) - \frac{Q_0}{LE\mu\tau}\int_0^L \exp\left(-\frac{x}{E\mu\tau}\right) x dx. \tag{5}$$

Integrating (5) gives the well-known Hecht equation[5] normally used to fit the measured dependence of the charge signal Q versus the applied bias U to evaluate the $\mu\tau$ product

$$Q = Q_0 \frac{U\mu\tau}{L^2}\left(1 - \exp\left(-\frac{L^2}{U\mu\tau}\right)\right). \tag{6}$$

Equation (6) is sensitive to the $\mu\tau$ product when

$$\frac{U\mu\tau}{L^2} \leq 1, \tag{7}$$

indicating that the measurements must be taken at low biases for high $\mu\tau$ material, while in order to evaluate Q_0, a single data point measured at high (maximum) bias will be sufficient. For example, for a typical 2-mm-thick device with a $\mu\tau$ product of $\sim 10^{-3}$ cm^2/V, the low-bias range can be extended up to 200 V, thereby giving sufficient data points to achieve high confidence in the quality of the fitting results. However, if the $\mu\tau$ product is 10^{-2} cm^2/V, the useful bias range is limited to only 20 V, wherein the measurements might be affected by several other effects, such as the nonuniformity of the electric field, diffusion, ballistic deficit, and a low signal-to-noise ratio.

If the electric-field strength is not uniform, Equation (6) must be modified. Let us assume for simplicity that the electric field strength decreases as a linear function from the cathode towards the anode

$$E = E_1 - \alpha x. \tag{8}$$

In reality, this dependence could be more complicated but for these model calculations, a linear dependence will be sufficient to illustrate our point. Then we can describe the drift velocity V as

$$V = \mu(E_1 - \alpha x). \tag{9}$$

From here, we find the time required for the electron cloud to travel a distance X measured from the cathode to be given by

$$t = \frac{1}{\mu\alpha}\ln\left(\frac{E_1}{E_1 - \alpha x}\right). \tag{10}$$

The total drift time is described by

$$t = \frac{1}{\mu\alpha}\ln\left(\frac{E_1}{E_2}\right), \tag{11}$$

where E_2 is the electric field at the anode. E_1 and E_2 are related as

$$\frac{E_1 + E_2}{2} = \frac{U}{L}. \tag{12}$$

To compare the results of the drift-time method and the conventional Hecht's method, we fabricated a $6 \times 6 \times 2$ mm^3 CZT sample cut from the same area of the same wafer, which we used for making 40-mm-long detectors. We collected a set of pulse-height spectra using a ^{241}Am source at biases ranging from 1 to 300 V. During the measurements, the detector was placed inside a standard eV Product's holder connected to a preamplifier box. The output signals of the preamplifier were shaped by an ORTEC 672 Spectroscopy Amplifier. We used

the bipolar shaping with a shaping time of 6 μs. The 59.6-keV photopeak was fitted to a Gaussian function to evaluate a dependence of the photopeak positions on the applied bias—a standard procedure used for measuring the $\mu\tau$ product. Application of the Hecht equation to the above dependence over the whole bias-voltage range did not result in a good fit as expected. By skipping the low bias points, one by one, we found that if we started the fitting from 18 V, the fitting gives statistically valid results. For the lowest starting point of 18 V, we obtained $\mu\tau = 2.3 \times 10^{-2}$ cm^2/V, which is consistent with typical values reported for the highest-quality detector grade CZT materials. However, this value is an order of magnitude smaller than that measured in this work. Moving the starting points to the higher biases for the fit resulted as expected in a continuously increasing $\mu\tau$ product, eventually approaching 0.3 cm^2/V. However, this does not mean that it is the correct $\mu\tau$ value. It only means that the Hecht equation is not sensitive to the $\mu\tau$ product when the voltage is somewhere above 50 V for a 2-mm-thick sample. (Any value between 0.02 and 0.3 cm^2/V gives an equally good fit.) In order to obtain valid estimates for the CZT material with high $\mu\tau$ products $>10^{-2}$ cm^2/V, one has to extend the fitting range well below 10 V (for a 2-mm-thick sample), where the measurements suffer from systematic errors. In other words, the Hecht equation cannot provide reliable estimates for the absolute values of the $\mu\tau$ products when the electron lifetimes exceed 10^{-2} cm^2/V. Of course, this does not prevent us from using the Hecht equation for comparative evaluations of CZT quality when absolute values are not important. Fig. 6(a) shows the measured dependence of the collected charge on the cathode bias (squares) on a semi-logarithm scale. For comparison, the two solid lines represent the fitting results corresponding to two different $\mu\tau$ products: 0.024 cm^2/V (bottom) and 0.1 cm^2/V (top). The latter value corresponds to our measured value for the tested samples.

As seen, there is a large discrepancy between the measured and modelled curves in the low bias region. As discussed above, the measurements at low biases can be affected by the electric field non-uniformity. It is also affected by the ballistic deficit, which reduces the amplitudes of the shaped signals when the rise time of the input signals becomes comparable to or less than the amplifier's shaping time. We demonstrate below that these two effects are sufficient to explain the observed discrepancy. First, we consider the effect of the electric field non-uniformity.

We assume that the electric field decreases linearly from the cathode towards the anode, as described in (8), which leads to Equation (11) for electron drift time. The latter equation can be used to evaluate a dependence of the slope of the electric field's strength coefficient (the parameter α in (8)) if its experimental dependence is known. For this purpose, we measured the drift time of the electron clouds by capturing the signal waveforms generated by a collimated alpha-particle source placed 2 mm above the cathode. We employed a digital oscilloscope for these measurements. The starting points of the charge signals can be easily identified, but the point corresponding to the cloud arrival time is not well defined, especially at low biases. Thus, to determine this point, we used linear extrapolations of the leading and saturated slopes of the signals and took the intersections of these lines as the arrival points. It is clear that this procedure is not the best for accurate drift-time measurements, but it is well suited for the illustrative purposes of this exercise. Fig. 7(a) shows the relationship between the drift times measured at different biases between 1 and 300 V and the calculated drift times assuming the uniform electric field and the electron mobility of 1000 cm^2/V s. The solid line represents the linear dependence of the drift time on the cathode bias. As seen, the measured drift time starts to deviate from the linear dependence on the cathode bias above $\sim$1 μs, which corresponds to the region below $\sim$50 V. For each measured point, we solved Equation (9) to find the value of the slope for a particular cathode bias. Fig. 7(b) depicts examples of the internal electric-field profiles (at four cathode biases 10, 20, 30, and 40 V) corresponding to the evaluated slopes. The dependence of the slopes on the applied bias allows us to evaluate the electric-field profiles, which can be substituted into Equation (5) to evaluate numerically the charge collection dependence, which now takes into account the electric-field variations inside the detector. The evaluated dependence is shown in Fig. 7(c) together with the curve calculated using the original Hecht equation. For both curves, we assumed the electron $\mu\tau$ value to be 0.1 cm^2/V. In other words, Fig. 7(c) illustrates an additional decrease of the collected charge if the electric field is not uniform.

The second effect in these estimates is from ballistic deficit. We measured the response function of the spectroscopy

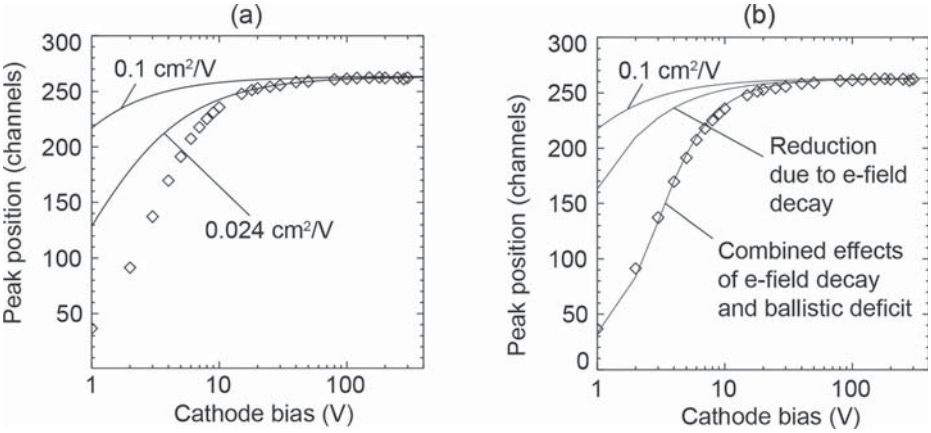

FIG. 6. (a) Measured dependence of the collected charge on the cathode bias (squares). The solid lines represent the fitting results corresponding to the two magnitudes of the $\mu\tau$ products: 0.024 cm^2/V (bottom) and 0.1 cm^2/V (top). (b) The reduction of the charge collection efficiency caused by the non-uniformity of the electric field only, and by the combined effects of the non-uniformity of the electric field and the ballistic deficit (see the text for detailed explanations). The detector's thickness is 2 mm.

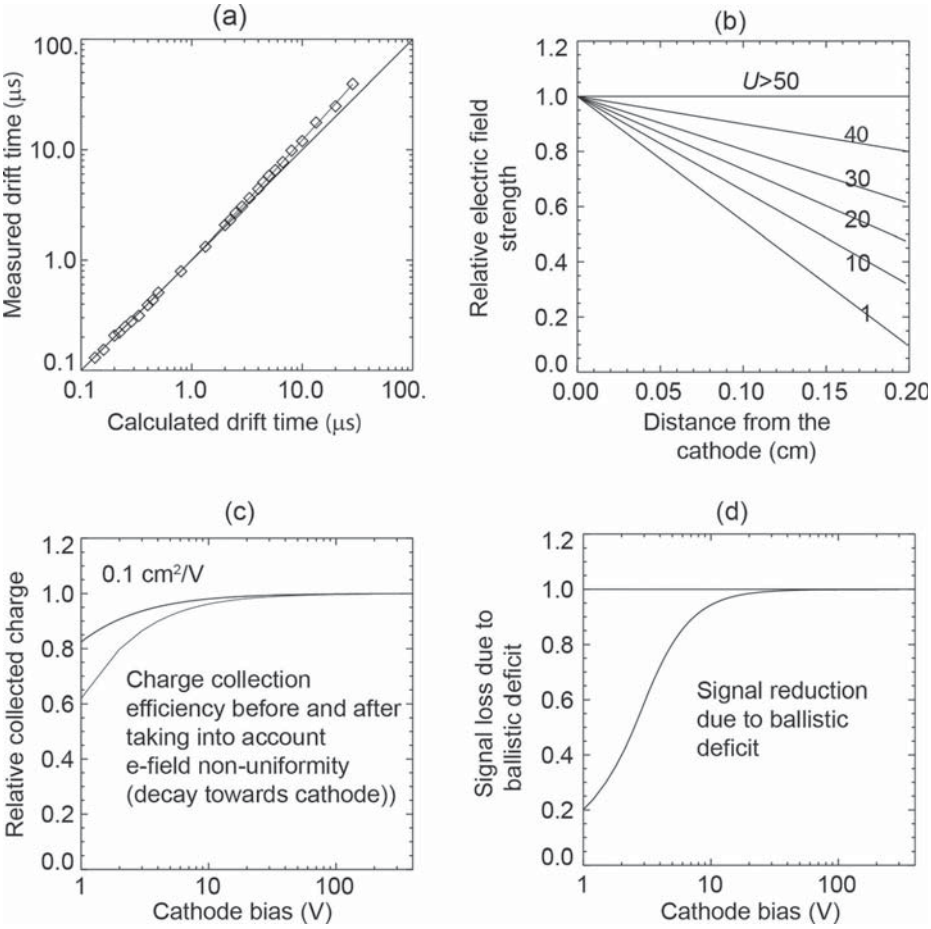

FIG. 7. (a) The drift times, measured at different biases between 1 and 300 V, plotted versus the calculated drift times, assuming a uniform electric field and an electron mobility of 1000 cm^2/V s. The solid line represents the linear dependence of the drift time on the cathode bias. (a) The signal reduction due to ballistic deficit on the applied bias evaluated for the experimental conditions used in these measurements; (b) the electric-field profiles evaluated for the four cathode biases 10, 20, 30, and 40 V; (c) A decrease of the charge collection efficiency after taking into account the decay of the electric field inside the detector; and (d) A decrease of the output signal amplitude due to the ballistic deficit effect (bipolar shaping with the 6-μs shaping time).

amplifier directly with an oscilloscope using a Gaussian approximation. We found that the Gaussian shaping time of the amplifier is 7.9 μs. Using the evaluated slopes of the electric field at different voltages, $\alpha(U)$, and substituting Equation (9) into (5), we can find the time dependence of the anode current generated by the electron cloud. By convoluting the currents with the amplifier response function, we can model the output signals (after the shaping amplifier) and calculate their amplitude reductions due to the ballistic deficit at different cathode biases and for the experimental conditions used in these measurements. As shown in Fig. 7(d), a significant reduction of the output signals is expected for our measurements at low biases of <20 V.

These calculations are depicted in Fig. 6(b), which illustrates the reduction of the charge-collection efficiency caused by non-uniformity of the electric field and the combined effects of the non-uniformity of the electric field and the ballistic deficit. The top solid line represents the expected dependence of the charge-collection efficiency calculated by using the Hecht equation with a $\mu\tau$ product of 0.1 cm^2/V. The second line represents the charge-collection efficiency after including the electric-field profiles evaluated from the drift-time measurements. The third line, which fits the experimentally measured points, represents the same dependence after including both effects into the Hecht equation. The fitting with a $\mu\tau$-product value of $\sim$0.1 cm^2/V is very close to the measured value by the drift-time method.

The fact that after applying all these corrections we obtain such a good agreement is almost unexpected. The main purpose of the above modeling exercise was to demonstrate that the ballistic deficit and non-uniformity of the electric field are sufficient to explain significant discrepancies of the simulated and experimental charge-collection efficiency at low voltage bias. In turn, this explains why using the Hecht equation fitting to evaluate the $\mu\tau$ product in CZT detectors gives significantly underestimated values, particularly for a high mobility-lifetime material. Other factors, such as the electron diffusion and surface recombination, may further reduce the charge collection efficiency at low biases.

IV. CONCLUSIONS

We applied the drift-time method to evaluate the $\mu\tau$ product in 40-mm-thick CZT samples. The measured values were found to be >0.1 cm^2/V, one order of magnitude higher than the values previously reported for the best CZT material. This can be explained by the fact that the Hecht equation fitting results used in previous measurements are affected by systematic errors caused by the non-uniformity of the electric field and the ballistic deficit. The drift-time method as applied in this case to thick, >1 cm, CZT detectors is an excellent way to correctly evaluate the electron lifetimes in a high-grade CZT material with a $\mu\tau$ product $>10^{-2}$ cm^2/V, yielding results for the electron lifetime that

are much more accurate than results obtained by fitting to the Hecht equation.

ACKNOWLEDGMENTS

This work was supported by the U.S. Department of Energy, Office of Nonproliferation Research and Development. The manuscript has been authored by Brookhaven Science Associates, LLC under Contract No. DE-SC0012704 with the U.S. Department of Energy. The United States Government retains, and the publisher, by accepting the article for publication, acknowledges, a world-wide license to publish or reproduce the published form of this manuscript, or allow others to do so, for the United States Government purposes.

[1]K. Hecht, "Zum Mechanismus des lichtelektrischen Primärstromes in isolierenden Kristallen," Z. Phys. **77**, 235–245 (1932).

[2]G. Knoll, *Radiation Detection and Measurement*, 3rd ed. (Wiley, New York, 2000), p. 480.

[3]Z. He, G. F. Knoll, and D. K. Wehe, "Direct measurement of product of the electron mobility and mean free drift time of CdZnTe semiconductors using position sensitive single polarity charge sensing detectors," J. Appl. Phys. **84**, 5566–5569 (1998).

[4]A. E. Bolotnikov and B. D. Ramsey, "Purification techniques and purity and density measurements of high-pressure Xe," Nucl. Instrum. Methods Phys. Res., Sect. A **383**, 619–623 (1996).

[5]S. Amerio, S. Amoruso, M. Antonello, P. Aprili *et al.*, "Design, construction and tests of the ICARUS T600 detector," Nucl. Instrum. Methods Phys. Res., Sect. A **527**, 329–410 (2004).

[6]A. E. Bolotnikov, G. S. Camarda, E. Chen, S. Cheng, Y. Cui, R. Gul, R. Gallagher, V. Dedic, G. De Geronimo, L. Ocampo Giraldo, J. Fried, A. Hossain, J. M. MacKenzie, P. Sellin, S. Taherion, E. Vernon, G. Yang, U. El-Hanany, and R. B. James, "CdZnTe position-sensitive drift detectors with thicknesses up to 5 cm," Appl. Phys. Lett. **108**, 093504 (2016).

[7]A. E. Bolotnikov, G. S. Camarda, G. A. Carini, M. Fiederle, L. Li, G. W. Wright, and R. B. James, "Performance studies of CdZnTe detector by using a pulse-shape analysis," Proc. SPIE **5922**, 59200K (2005).